Electrochemical oxidation of propylene carbonate (containing various salts) on aluminium electrodes

Kiyoshi Kanamura, Takashi Okagawa, Zen-ichiro Takehara

Division of Energy and Hydrocarbon Chemistry, Graduate School of Engineering, Kyoto University, Yoshida-honmachi, Sakyo-ku, Kyoto 606-01, Japan

Abstract

Electrochemical reactions taking place on aluminium electrodes in propylene carbonate, with 1.0 M $LiClO_4$, $LiBF_4$, or $LiPF_6$, are investigated in terms of the stability of non-aqueous electrolytes. The techniques used are potential sweep method, X-ray photoelectron spectroscopy, and in situ Fourier-transform infrared (FT-IR) spectroscopy. From these analysis, it is found that the surface of the aluminium electrode is covered with aluminium oxides and fluorides as a passivation layer when it is polarized at 5.5 V versus Li/Li^+. Moreover, the surface state of the aluminium electrode depends on the type of electrolyte salt, as do the current–potential curves. On the other hand, in situ FT-IR studies indicate that the oxidation products of propylene carbonate are independent of the type of electrolyte salt. From these results, it is concluded that the stability of propylene carbonate electrolyte depends on the surface state of the aluminium electrode which is strongly combined with the stability of anions.

Keywords: Rechargeable lithium batteries; Electrolytes; Aluminium; Capacitor; Non-aqueous electrolytes

1. Introduction

Researches on rechargeable lithium batteries have been performed extensively for new applications, such as electric vehicles and load-levelling systems. To realize these applications, the batteries must have high energy and power densities. Rechargeable lithium batteries are promising candidates, while most traditional batteries do not have sufficient performance. The high performance of rechargeable lithium batteries is provided by their high discharge potential. This results from the use of material that have more potential as anodes (lithium metal or carbon materials) and cathodes (transition metal), respectively. Recently, a cell voltage of 4.0 V (i.e., almost twice as high as that of lead/acid batteries) has been achieved by using $LiCoO_2$, $LiNiO_2$ and $LiMn_2O_4$ as cathodes and lithium or carbon as anodes. When these batteries are charged at a constant current, the cell voltage rises above 4.0 V. Therefore, oxidation of the electrolyte is a critical factor for the battery performance, as well as the reduction of electrolyte by lithium anodes or other anode materials that have a similar potential to lithium metal. Oxidative or reductive decomposition of non-aqueous electrolytes is a very important safety feature of rechargeable lithium batteries. The reduction of non-aqueous electrolytes has been

studied extensively [1–7], and connected to the rechargeability of the lithium metal and carbon anodes. Similarly, the electrochemical oxidation of non-aqueous electrolytes has also been investigated [8–15]. In these studies, platinum or nickel electrodes have been used as the working electrodes. Some other materials have been utilized in rechargeable lithium batteries as current collectors [16] and, accordingly, the electrochemical oxidation of non-aqueous electrolytes on such materials is important for practical battery technology.

The electrochemical oxidation of non-aqueous electrolytes also holds interest for other electrochemical applications (e.g., organic electrochemistry). Consequently, the electrochemical oxidation of acetonitrile or propylene carbonate containing $LiClO_4$ on platinum electrodes has been investigated using several in situ analytical methods [17–19]. These studies showed that the oxidation of anions took place before the oxidation of solvents [20–24]. Therefore, the type of anion is an important factor for the electrochemical oxidation of non-aqueous electrolytes.

In this study, the electrochemical oxidation of propylene carbonate containing various electrolyte salts on aluminium electrodes (which has been used as current collector in rechargeable lithium batteries) was examined using several analytical methods.

2. Experimental

Propylene carbonate (PC) with 1.0 M $LiClO_4$, $LiBF_4$, or $LiPF_6$ ($LiClO_4$/PC, $LiBF_4$/PC, and $LiPF_6$/PC) was used as the electrolyte. The electrolytes were purchased from Mitsubishi Chemical Co. and had a water content of <20 ppm. The electrochemical oxidation of these electrolytes was investigated using in situ Fourier-transform infrared (FT-IR) spectroscopy. The electrochemical cell for the in situ FT-IR spectroscopy used in this study has been described previously [25]. The normalized difference between two power spectra at two different electrode potentials ($\Delta R/R$) was calculated according to the following equation:

$$\frac{\Delta R}{R} = \frac{R_{E_{i+1}} - R_{E_i}}{R_{E_i}} \quad (1)$$

The electrode potential was set at an initial potential, E_i, for several tens of minutes to obtain a flat and smooth background which is important to get a high-quality spectrum. The electrode potential was then changed from the initial potential to another value (E_{i+1}) that was more anodic. The in situ FT-IR measurement was performed after several minutes. The power spectrum at the initial potential (E_i) was subtracted from that at the potential of E_{i+1} to obtain the differential FT-IR spectrum, then the differential spectrum was divided by the power spectrum at E_i to normalize the spectrum. After 10 minutes, the potential was stepped from E_{i+1} to a more anodic potential than E_{i+1} (E_{i+2}). The FT-IR spectrum was measured again after several minutes rest. The normalized differential FT-IR spectrum at E_{i+2} was calculated from that at E_{i+1} and E_{i+2}. These products were repeated in the electrode potential range 4.0 to 8.0 V versus Li/Li^+ with a potential-step experiment (0.2 V potential width). The working electrode was a cylindrical rod of aluminium, as shown in Fig. 1. The sidewall was sealed by a Teflon® tape to avoid the electrochemical oxidation of non-aqueous electrolytes. The electrode surface was polished with fine alumina powders to obtain a mirror surface that had adequate reflectivity for IR measurement. Nickel wire was used as the counter electrode and lithium metal (Honjo Metal Co., Ltd.) as the reference electrode. Assembly of the FT-IR cell was performed under an argon atmosphere. It was then transferred to
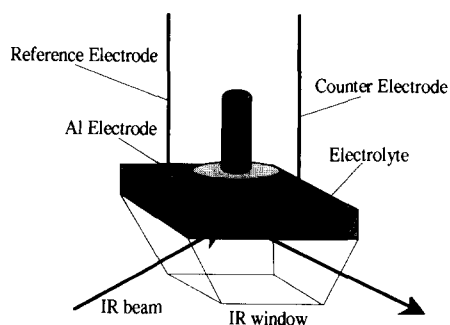
a FT-IR spectrometer. The cell can be tightly sealed to avoid effects of air atmosphere. The atmosphere in an analysis chamber of the FT-IR spectrometer was air dried by $CaCl_2$. Therefore, the peak intensity of CO_2 includes some uncertainty.

Current–potential curves in the three electrolytes were measured by linear potential sweep voltammetry at 50 mV s^{-1}. Aluminium plates were used as the working electrode and lithium metal as the counter and reference electrodes. All potentials are reported with respect to the Li/Li^+ electrode. The electrolytes were the same as these employed in the in situ FT-IR measurements. The experiments were again performed under an argon atmosphere at room temperature.

3. Results and discussion

Fig. 2 shows the current–potential curves for the electrochemical oxidation of $LiClO_4$/PC, $LiBF_4$/PC or $LiPF_6$/PC on aluminium electrodes. In the potential range 3.0 to 5.0 V, a small current (<0.1 mA cm^{-2}) was observed in all the current –potential curves. At potentials above 5.0 V, the features of the current–potential curves in $LiClO_4$/PC were markedly different from those in $LiBF_4$/PC or $LiPF_6$/PC, as follows. An anodic current peak was observed in $LiClO_4$/PC, but not in $LiBF_4$/PC or $LiPF_6$/PC. The anodic current in $LiBF_4$/PC increased slightly with the anodic potential sweep. This behaviour was not observed in $LiPF_6$/PC. These results suggest that electrochemical reactions taking place on the aluminium electrode depend on the type of electrolyte salt. Probably, anions are strongly related to the electrochemical reactions that occur on the aluminium electrode. It has been reported [20–22] that anions can be oxidized at a more cathodic potential than the on-set potential for the electrochemical oxidation of PC. The oxidation products of the anions (which were detected by in situ electron spin resonance techniques) were assigned to some radical species that had a high reactivity with the solvents or electrode materials. These results were obtained with platinum electrodes. It is likely that the oxidation of PC is preceded by the electrochemical oxidation of anions, even when using aluminium electrodes.

On the other hand, aluminium electrodes can be oxidized to form surface films. Therefore, the electrochemical oxida-
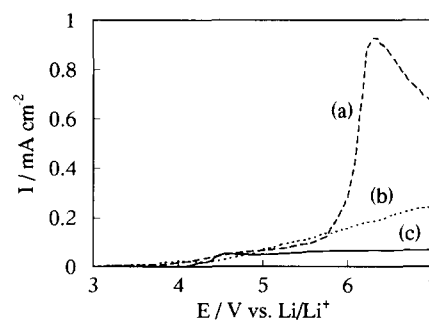

Fig. 1. Schematic of in situ FT-IR measurement for electrochemical oxidation of non-aqueous electrolytes on an aluminium electrode.

Fig. 2. Current–potential curves for potential sweep from 3.0 to 7.0 V at 50 mV s^{-1} in: (a) $LiClO_4$/PC; (b) $LiBF_4$/PC, and (c) $LiPF_6$/PC.
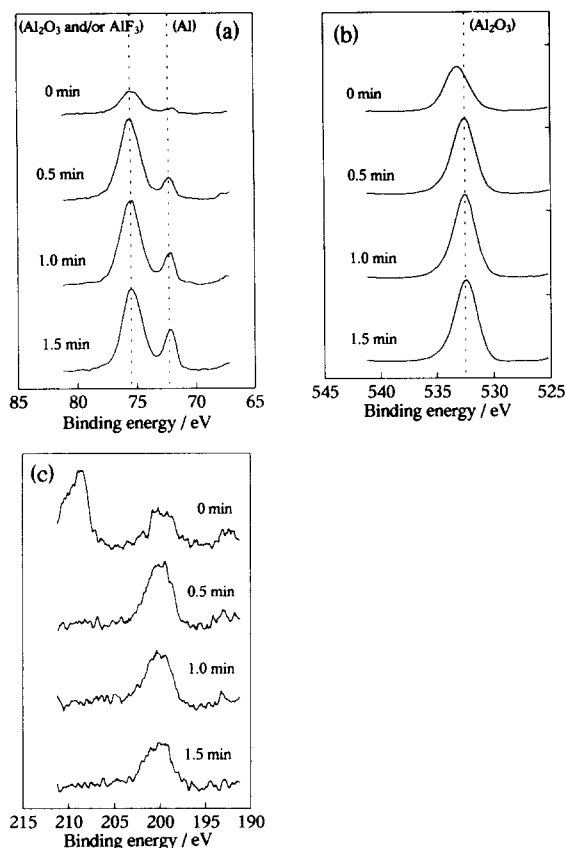
Fig. 3. XPS spectra of (a) Al(2p), (b) O(1s), and (c) Cl(2p) for aluminium electrode polarized at 5.5 V vs. Li/Li⁺ for 1 h in LiClO₄/PC; time periods (min) indicate duration of the argon ion etching.

tion behaviour on aluminium electrodes is different from that on platinum electrodes in terms of the surface state. Moreover, the electrochemical oxidation of anions may also be related to the formation of the surface film. If the surface film depends on the anion type, electrochemical reactions on aluminium electrodes are also influenced by the nature of the electrolyte salts. Therefore, electrochemical oxidation of non-aqueous electrolytes has to be investigated in terms of the surface change of the electrode combined with the oxidation of anions. In this study, the change of the electrode surface state was investigated using X-ray photoelectron spectroscopy (XPS), while the decomposition products of PC were detected using in situ FT-IR measurement.

Fig. 3 shows the XPS spectra of Al(2p) and O(1s) for the aluminium electrode surface which was oxidized at 5.5 V versus Li/Li⁺ in LiClO₄/PC for 1 h. In the XPS pattern of Al(2p), the two peaks observed at 72.3 and 75.5 eV probably correspond to aluminium and Al₂O₃, respectively. In the XPS pattern of O(1s), a peak is found at 532.5 eV; this is attributed to Al₂O₃. In the XPS pattern of Cl(2p), two peaks are observed at 210 and 200 eV, respectively. These peaks are assigned to ClO₄⁻ and Cl⁻, respectively. The presence of aluminium and Al₂O₃ peaks in the XPS spectra of Al(2p) before and after argon ion sputtering suggest that only a part of the aluminium electrode surface is covered with a thick

surface film of Al₂O₃, while other parts are covered with very thin aluminium oxides.

Fig. 4 shows the depth profile of each element in a molar ratio that can be calculated by the cross section for the ionization of each element and the integrated peak intensity for these elements. The molar ratios of all elements are almost constant in the sputtering time range from 0.5 to 1.5 min. A small amount of elemental chlorine is involved in the surface film on the aluminium electrode. The presence of Cl⁻ ions is explained only by the electrochemical oxidation of ClO₄⁻ ions. Though the main species can be expected to be aluminium oxides, the aluminium content in the surface film was larger than the oxygen content, assuming that Al₂O₃ is formed in the surface film. Since the presence of Al²⁺ and Al⁺ ions is unusual, the molar ratio between aluminium and oxygen is due to the simultaneous detection of aluminium and Al₂O₃ by XPS, as shown in Fig. 3. This fact can be explained by a large distribution in the thickness of the surface film.

Fig. 5 shows the XPS pattern of Al(2p), O(1s), and F(1s) for the aluminium electrode after polarization at 5.5 V versus Li/Li⁺ in LiPF₆/PC. A peak is observed at 75.5 eV in the XPS pattern of Al(2p). This binding energy corresponds to fluorides and/or oxides of aluminium. The peak is similar to that in the XPS pattern of Al(2p) for the aluminium electrode anodically polarized in LiClO₄/PC. On the other hand, the peak corresponding to aluminium metal is not observed in this Al(2p) spectra. This result indicates that the electrode surface is fully covered with aluminium compounds and is different from that for LiClO₄/PC. A peak is observed at 532.5 eV in the XPS pattern of O(1s) and the peak intensity does not decrease with argon ion etching. In the XPS pattern of F(1s), a peak is found at 686.5 eV. This peak corresponds to aluminium fluorides and, therefore, indicates the presence of aluminium fluorides in the surface film. From these results, it can be seen that the electrode surface is covered with aluminium oxides and fluorides. The F element involved in the surface film is probably derived from the decomposition of the anions. This means that anions decompose during anodic polarization of the aluminium electrode. Fig. 6 shows the depth profile of each element in a molar ratio. The molar ratios are not changed by the argon ion sputtering. The alu-
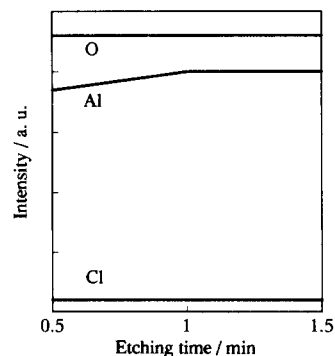

Fig. 4. Depth profiles of O, Al and Cl elements in surface film of an aluminium electrode polarized at 5.5 V vs. Li/Li⁺ for 1 h in LiClO₄/PC.
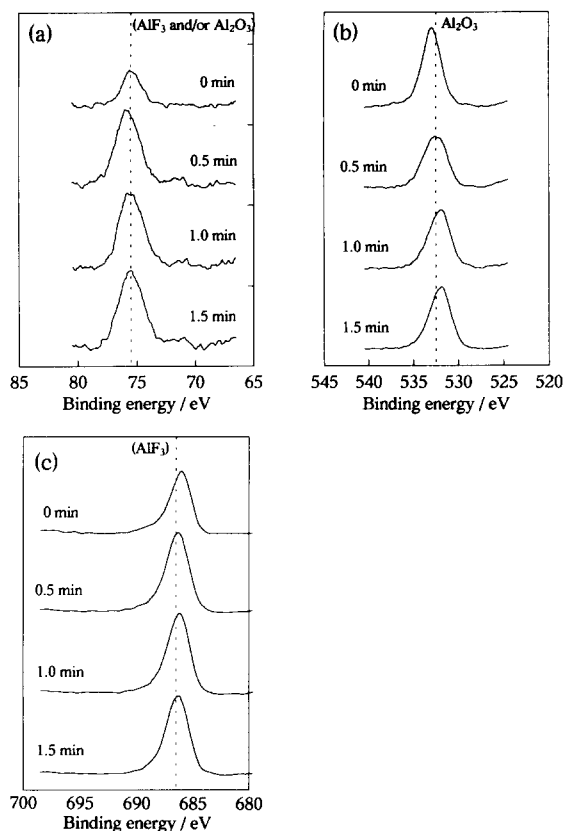
　　　　　　　　　K. Kanamura et al. / Journal of Power Sources 57 (1995) 119–123

Fig. 5. XPS spectra of (a) Al(2p), (b) O(1s), and (c) F(1s) for aluminium electrode polarized at 5.5 V vs. Li/Li$^+$ for 1 h in LiPF$_6$/PC; time periods (min) indicate duration of argon ion etching.
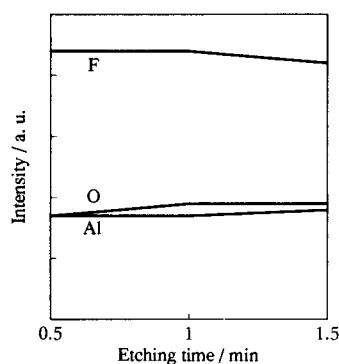

Fig. 6. Depth profiles of O, Al and Cl elements in surface film of an aluminium electrode polarized at 5.5 V vs. Li/Li$^+$ for 1 h in LiPF$_6$/PC.

minium content in the surface film is reasonable, compared with the total content of O and F, assuming that Al$_2$O$_3$ and AlF$_3$ are formed on the aluminium electrode. This indicates that the whole surface is covered with a thick layer that consists of Al$_2$O$_3$ and AlF$_3$.

The anodic oxidation behaviour of aluminium electrodes in these two electrolytes suggests that the physical and chemical properties of the surface film depends on the type of electrolyte salt. The surface formed in LiClO$_4$/PC is neither dense nor thick, but that formed in LiPF$_6$/PC is both thick and tight. Since the electrochemical oxidation of the non-aqueous electrolyte occurs on the electrode surface, the

formation of aluminium compounds influences the electrochemical oxidation of PC. As shown in the current–potential curves, PC decomposition depends on the type of electrolyte salt. The electrochemical reaction giving the anodic current has not yet been determined. In this study, the electrochemical oxidation products were detected using in situ FT-IR measurements.

Fig. 7 shows the normalized differential spectra for the electrochemical oxidation of LiClO$_4$/PC on the aluminium electrode. The upward peaks in the normalized differential spectra correspond to a consumption of compounds, and the downward peaks show the production of chemical species due to the anodic oxidation of PC. No significant peaks were observed in the potential region from 3.0 to 4.6 V. At 4.8 V, several peaks corresponding to electrochemical oxidation products of the electrolytes were observed, but their intensities were weak. At 5.0 V, the peak intensities increased considerably; this indicated that the electrochemical oxidation rate of PC was accelerated at this potential. In the potential region from 5.2 to 7.0 V, no significant peaks were observed in the normalized differential spectra, and this suggested that the electrochemical oxidation rate was kept at constant value. Beyond 7.2 V, all peak intensities increased with sweeping electrode potential in the positive-going direction.

Fig. 8 displays the normalized differential spectra for the electrochemical oxidation of LiBF$_4$/PC on an aluminium electrode. At 5.4 V, several small peaks appeared in the spectra. Their intensities remained unchanged in the potential region between 5.4 and 6.0 V, and then increased as the potential was taken beyond 6.0 V. Therefore, the rising anodic current beyond 5.4 V in Fig. 2 corresponds to the electrochemical oxidation of PC. The on-set potential for the anodic oxidation in this electrolyte (5.4 V) was more anodic than that in LiClO$_4$/PC.

Fig. 9 shows the normalized differential spectra for the electrochemical oxidation of LiPF$_6$/PC on an aluminium electrode. Using in situ FT-IR spectroscopy, oxidation of PC was not observed at potentials more cathodic than 5.4 V. A
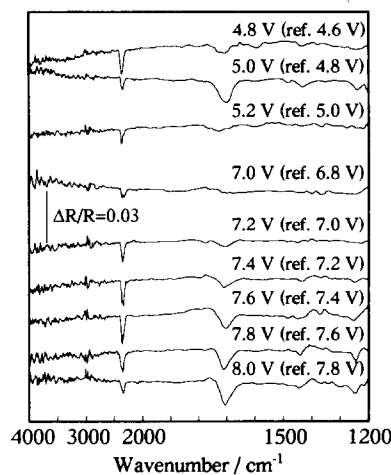

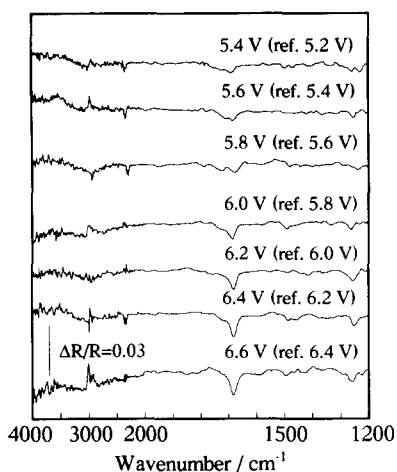Fig. 7. Normalized differential spectra obtained during anodic polarization from 4.8 to 8.0 V vs. Li/Li$^+$ in LiClO$_4$/PC.

Fig. 8. Normalized differential spectra obtained during anodic polarization from 4.8 to 8.0 V vs. Li/Li$^+$ in LiBF$_4$/PC.
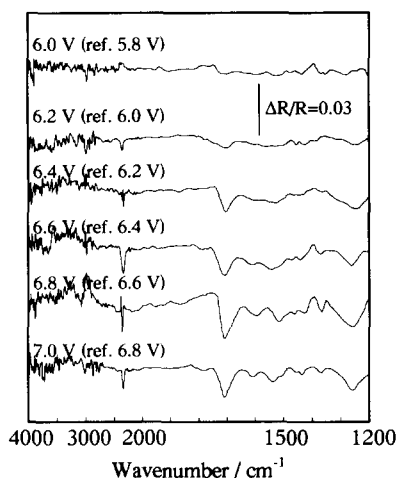

Fig. 9. Normalized differential spectra obtained during anodic polarization from 4.8 to 8.0 V vs. Li/Li$^+$ LiPF$_6$/PC.

small, steady-state, anodic current was observed in this potential region, however, as shown in Fig. 2. From these results, it can be seen that anodic current is not due to the oxidation of PC, but is caused by the oxidation of either the electrolyte salts or the electrodes. From comparison of the spectra, it is concluded that LiPF$_6$/PC is the most stable of the three PC electrolytes.

Several downward peaks are observed in the spectra of the three electrolytes. The wave number of these peaks are independent on the type of electrolyte salt. A peak at 1700 cm^{-1} corresponds to a C = O stretching vibration, some peaks observed in the wave number region from 1200 to 1600 cm^{-1} are assigned to C–O vibration in the carboxylic group. These wave numbers are shifted from those for the original PC. The peak shifts indicate that, at the initial step of the electrochemical oxidation of PC, a ring-opening reaction takes place to

form an intermediate adsorbed on the aluminium electrode surface.

From a comparison of the current–potential curves and the normalized differential spectra, it can be seen that the anodic current does not correspond to the oxidation of PC. When a nickel electrode is used as the working electrode, the current–potential curves correspond well with the normalized differential spectra, as reported previously [25]. This means that the anodic current is not only due to the electrochemical oxidation of PC, but is also caused by the electrochemical oxidation of the electrolyte salts and the electrodes. When LiClO$_4$ was used as the electrolyte salt, the surface film formed on the aluminium electrode was not stable. This is also supported by XPS analysis, as discussed above.

References

[1] D. Aurbach, M. Darox, P. Faguy and E. Yeager, *J. Electroanal. Chem.*, *297* (1991) 225.
[2] D. Pletcher, J.F. Rohan and A.G. Ritchie, *Electrochim. Acta*, *39* (1994) 2015.
[3] S.A. Campbell, C. Bowes and R.S. McMillan, *J. Electroanal. Chem.*, *284* (1990) 195.
[4] M. Odziemkowski and D.E. Irish, *J. Electrochem. Soc.*, *140* (1993) 1546.
[5] D. Aurbach and O. Chosid (Youngman), *J. Electrochem. Soc.*, *140* (1993) L1.
[6] K. Kanamura, H. Tamura, S. Shiraishi and Z. Takehara, *J. Electroanal. Chem.*, in press.
[7] D. Aurbach, Y. Ein-Eli, O. Chosid, Y. Catmeli, M. Babai and H. Yamin, *J. Electrochem. Soc.*, *141* (1994) 603.
[8] F. Ossala, G. Pistoia, R. Seeber and P. Ugo, *Electrochim. Acta*, *33* (1988) 47.
[9] S. Tobishima and T. Okada, *Electrochim. Acta*, *30* (1985) 1715.
[10] A.N. Dey and E.J. Rudd, *J. Electrochem. Soc.*, *121* (1974) 1249.
[11] S. Nakahama, S. Hino and N. Yamazaki, *Polymer J.*, *2* (1971) 56.
[12] P. Novak and W. Vielstich, *J. Electrochem. Soc.*, *137* (1990) 1681.
[13] M.G.S.R. Thomas, P.G. Bruce and J.B. Goodenough, *J. Electrochem. Soc.*, *132* (1985) 1522.
[14] M. Alamgir, R.D. Moulton and K.M. Abraham, *Electrochim. Acta*, *36* (1991) 773.
[15] D. Vofsi and A.V. Tobolsky, *J. Polymer Science*, *3* (1965) 3261.
[16] D. Guyomard and J.M. Tarascon, *J. Power Sources*, *54* (1995) 92; S. Yamada, M. Fujiwara and M. Kanda, *J. Power Sources*, *54* (1995) 207; H. Abe, K. Zaghib, K. Tatsumi and S. Higuchi, *J. Power Sources*, *54* (1995) 236; L.P.L.M. Pabon and A. Roskam, *J. Power Sources*, *54* (1995) 316.
[17] G. Eggert and J. Heitbaum, *Electrochim. Acta*, *31* (1986) 1443.
[18] B. Rasch, E. Cattaneo, P. Novak and W. Vielstich, *Electrochim. Acta*, *36* (1991) 1397.
[19] P. Novak, P.A. Christensen, T. Iwashita and W. Vielstich, *J. Electroanal. Chem.*, *263* (1989) 37.
[20] A.H. Maki and D.H. Geske, *J. Chem. Phys.*, *30* (1959) 1356.
[21] V.R. Koch and L.L. Miller, *J. Electroanal. Chem.*, *43* (1973) 318.
[22] D.B. Clark, M. Fleishmann and D. Pletcher, *J. Electroanal. Chem.*, *42* (1973) 133.
[23] M. Fleishmann and D. Pletcher, *Tetrahedron*, *60* (1968) 6255.
[24] G. Tourillon, P.C. Lacaze and J.E. Dubois, *J. Electroanal. Chem.*, *100* (1979) 247.
[25] K. Kanamura, S. Toriyama, S. Shiraishi and Z. Takehara, *J. Electrochem. Soc.*, *142* (1995) 1383.